A Microwave Measurement Procedure for a Full Characterization of Ortho-Mode Transducers

Oscar Antonio Peverini, Riccardo Tascone, Augusto Olivieri, Massimo Baralis, Renato Orta, *Senior Member, IEEE*, and Giuseppe Virone

***Abstract*—Ortho-mode transducers (OMTs) are key components in both dual-polarized antenna feed systems for telecommunication and radio-astronomy applications. The evaluation of the overall system performance requires the measurement of the return loss, isolation, and cross-coupling levels of the OMTs. In this paper, a novel technique for the microwave measurements of the full 4×4 scattering matrix of such devices is reported, which is based on different measurements at the single-polarized ports.**

***Index Terms*—Measurement techniques, microwave components, ortho-mode transducers (OMTs), waveguide devices.**

I. Introduction

ORTHO-MODE transducers (OMTs) are waveguide components used to select orthogonally polarized modes propagating in a circular or square waveguide, usually called common port [1], [2]. The full characterization of OMTs by means of their 4×4 scattering matrix is required in order to evaluate the overall performance of dual-polarized antenna feed systems. OMTs are also key components in radiometers used in radio astronomy for the detection of the polarized sky emission [3], as in the Sky Polarization Observatory (SPOrt) project [4], where correlation radiometers are used to detect simultaneously the Q and U Stokes parameters. One figure-of-merit of a correlation radiometer is its rejection to the unpolarized emission. High rejections are obtained by means of OMTs exhibiting very low cross-coupling coefficients S_{14} and S_{23}, where S_{ij} are the scattering parameters of the OMT labeled according to Fig. 1, where ports 1 and 2 are directly coupled to ports 3 and 4, respectively.

OMTs with high performances require accurate measurements of all their scattering parameters. In [1], [5], and [6], the OMTs were experimentally characterized by measuring directly the return loss and the isolation at the single polarized ports. In [7], high levels of cross-couplings are reported as well, but the measurement conditions are not described. In order to derive a complete experimental characterization of the OMT, one could think to perform a measurement procedure similar to those applied in the calibration of network analyzers, as the thru-reflection-line (TRL) algorithm [8], [9]. In particular, the OMT could be regarded as the transition block used in the multimode TRL procedure described in [10]. This block relates one common multimode waveguide supporting N modes to N single-mode lines. A basic cornerstone of this procedure is the ordering of the eigenvalues corresponding to the phase delay of each mode in the common waveguide. Obviously, this can be accomplished only for nondegenerate modes, i.e., modes exhibiting different propagation constants. Unfortunately, this is not the case of interest. In fact, as far as OMTs are concerned, their common port is a square or circular waveguide supporting two degenerate modes. Hence, this technique is not applicable.

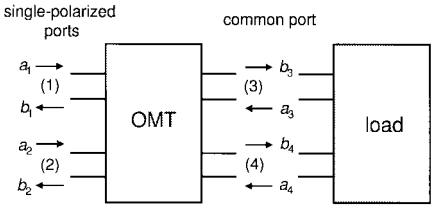

Fig. 1. Schematic representation of the OMT and generic load $\underline{\underline{\Gamma}}_{L,i}$ to be connected at the common port, which consists of two electrical ports (3) and (4). Ports 1 and 2 are directly coupled to electrical ports 3 and 4, respectively.

In this paper, a new procedure for the measurements of the full 4×4 scattering matrix of OMTs is proposed, which is based on the elaboration of five measurements at the single polarized ports, when the common waveguide is loaded with: 1) a matched load; 2) an unknown diagonal reactive load defining the two polarizations directions; 3) an ideal short circuit; and 4) and 5) the diagonal reactive load and the short circuit both shifted by a line of unknown length. Moreover, as far as the practical aspects are concerned, during the measurement sequence, the network analyzer cables are kept connected to the single-polarized ports, avoiding any movement of the cables, which degrades the measurement accuracy.

II. Theory

A. Measurement Activity

The measurement technique presented in this paper is based on a set of five 2×2 reflection measurements performed by means of a vectorial network analyzer connected to the two single-polarized ports (ports 1 and 2 in Fig. 1), when the common port is terminated with five different loads. The 2×2 reflection coefficient measured at the ports 1 and 2 can be expressed as [11]

$$\underline{\underline{\Gamma}}_i = \underline{\underline{S}}_{11} + \underline{\underline{S}}_{12} \cdot \left(\underline{\underline{\Gamma}}_{L,i}^{-1} - \underline{\underline{S}}_{22} \right)^{-1} \cdot \underline{\underline{S}}_{21} \qquad (1)$$

Manuscript received June 10, 2002; revised September 30, 2002. This work was supported by the Italian Space Agency (ASI).

The authors are with the Istituto di Elettronica e di Ingegneria dell'Informazione e delle Telecomunicazioni, Italian National Research Council, Dipartamento di Elettronica, Politecnico di Torino, 10129 Turin, Italy.

Digital Object Identifier 10.1109/TMTT.2003.809629

0018-9480/03$17.00 © 2003 IEEE

where $\underline{\underline{\Gamma}}_{L,i}$ is the 2×2 reflection coefficient of the load connected to the OMT common port and $\underline{\underline{S}}_{ij}$ are the 2×2 blocks of the 4×4 OMT scattering matrix

$$\begin{bmatrix} b_1 \\ b_2 \\ b_3 \\ b_4 \end{bmatrix} = \begin{bmatrix} \underline{\underline{S}}_{11} & \underline{\underline{S}}_{12} \\ \underline{\underline{S}}_{21} & \underline{\underline{S}}_{22} \end{bmatrix} \cdot \begin{bmatrix} a_1 \\ a_2 \\ a_3 \\ a_4 \end{bmatrix} \quad \begin{bmatrix} a_3 \\ a_4 \end{bmatrix} = \underline{\underline{\Gamma}}_{L,i} \cdot \begin{bmatrix} b_3 \\ b_4 \end{bmatrix} \tag{2}$$

being a_i and b_i $(i=1,\ldots,4)$ the incident and scattered power waves with respect to the OMT (see Fig. 1).

The first step is to measure the 2×2 $\underline{\underline{S}}_{11}$ block of the OMT. This can be performed by directly connecting a matched load $\left(\underline{\underline{\Gamma}}_{L,0}=0\right)$ to the common port. If a matched load with good performances is not available, these parameters can be measured by using any unknown dual-mode transition connected to the common port, as explained in the Appendix. Next, the four 2×2 reflection coefficients $\underline{\underline{\Gamma}}_i$ at ports 1 and 2 are measured by terminating the common port on the following four different loads $\underline{\underline{\Gamma}}_{L,i}$.

- $\underline{\underline{\Gamma}}_{L,1}$ is a reactive load, which is diagonal with respect to the basis formed by the two polarizations of interest. It is necessary that the phases of the reflection coefficients of the load corresponding to the two polarizations are different.
- $\underline{\underline{\Gamma}}_{L,2}$ is obtained by inserting an h-long waveguide between the common port and the reactive load $\underline{\underline{\Gamma}}_{L,1}$, i.e., $\underline{\underline{\Gamma}}_{L,2}=\underline{\underline{e}}^{-2\jmath\theta}\cdot\underline{\underline{\Gamma}}_{L,1}$, where $\underline{\underline{e}}^{-2\jmath\theta}$ is a diagonal matrix with $\theta_l=\beta_l h$, being β_l $(l=1,2)$ the longitudinal propagation constant of the two degenerate modes of the waveguide at the common port. Here, for generality, they are considered different.
- $\underline{\underline{\Gamma}}_{L,3}$ is a short circuit, i.e., $\underline{\underline{\Gamma}}_{L,3}=-\underline{\underline{I}}$, with $\underline{\underline{I}}$ denoting the 2×2 identity matrix.
- $\underline{\underline{\Gamma}}_{L,4}$ corresponds to the short circuit shifted by the h-long waveguide, i.e., $\underline{\underline{\Gamma}}_{L,4}=-\underline{\underline{e}}^{-2\jmath\theta}$.

On the basis of this set of measurements ($\underline{\underline{S}}_{11}$ and $\underline{\underline{\Gamma}}_i$ with $i=1,\ldots,4$), one can write

$$\underline{\underline{S}}_{22}=\underline{\underline{\Gamma}}_{L,i}^{-1}-\underline{\underline{S}}_{21}\cdot\underline{\underline{A}}_i^{-1}\cdot\underline{\underline{S}}_{12},\qquad i=1,\ldots,4 \tag{3}$$

where $\underline{\underline{A}}_i=\underline{\underline{\Gamma}}_i-\underline{\underline{S}}_{11}$ are measured and symmetric matrices. By equating the two expressions of $\underline{\underline{S}}_{22}$ corresponding to $i=m$ and $i=n$, one obtains the following equation:

$$\underline{\underline{S}}_{12}\cdot\left(\underline{\underline{\Gamma}}_{L,m}^{-1}-\underline{\underline{\Gamma}}_{L,n}^{-1}\right)^{-1}\cdot\underline{\underline{S}}_{12}^{T}=\left(\underline{\underline{A}}_m^{-1}-\underline{\underline{A}}_n^{-1}\right)^{-1}=\underline{\underline{B}}_{mn} \qquad \forall\, m,n=1,\ldots,4 \tag{4}$$

where $(\ldots)^T$ indicates the transposition operation. As in the multimode TRL technique [10], in order to evaluate the $\underline{\underline{S}}_{12}$ block, one could use the following three matrices:

$$\underline{\underline{B}}_{13}=\underline{\underline{S}}_{12}\cdot\left(\underline{\underline{I}}+\underline{\underline{\Gamma}}_{L,1}^{-1}\right)^{-1}\cdot\underline{\underline{S}}_{12}^{T} \tag{5}$$

$$\underline{\underline{B}}_{24}=\underline{\underline{S}}_{12}\cdot\left(\underline{\underline{I}}+\underline{\underline{\Gamma}}_{L,1}^{-1}\right)^{-1}\cdot\underline{\underline{e}}^{-2\jmath\theta}\cdot\underline{\underline{S}}_{12}^{T} \tag{6}$$

$$\underline{\underline{B}}_{43}=\underline{\underline{S}}_{12}\cdot\left(\underline{\underline{I}}-\underline{\underline{e}}^{2\jmath\theta}\right)^{-1}\cdot\underline{\underline{S}}_{12}^{T}. \tag{7}$$

In particular, the matrix $\underline{\underline{B}}_{13}$ is derived by combining the measurements corresponding to the reactive load $\underline{\underline{\Gamma}}_{L,1}$ and to the short circuit $\underline{\underline{\Gamma}}_{L,3}$, whereas $\underline{\underline{B}}_{24}$ corresponds to the reactive load and the short circuit, both set back by the h-long line ($\underline{\underline{\Gamma}}_{L,2}$ and $\underline{\underline{\Gamma}}_{L,4}$, respectively). Finally, $\underline{\underline{B}}_{43}$ refers to the measurements performed with the short circuit in the following two positions: directly connected $\left(\underline{\underline{\Gamma}}_{L,3}\right)$ and shifted by the h-long line $\left(\underline{\underline{\Gamma}}_{L,4}\right)$. At this point, one can note that

$$\underline{\underline{B}}_{24}\cdot\underline{\underline{B}}_{13}^{-1}=\underline{\underline{S}}_{12}\cdot\underline{\underline{e}}^{-2\jmath\theta}\cdot\underline{\underline{S}}_{12}^{-1} \tag{8}$$

so that the phase-delay matrix $\underline{\underline{e}}^{-2\jmath\theta}$ and $\underline{\underline{S}}_{12}$ block correspond to the eigenvalues $(\underline{\underline{\Lambda}})$ and eigenvectors $(\underline{\underline{U}})$ matrices of $\underline{\underline{B}}_{24}\cdot\underline{\underline{B}}_{13}^{-1}$, respectively, i.e.,

$$\underline{\underline{e}}^{-2\jmath\theta}=\underline{\underline{\Lambda}} \tag{9}$$

$$\underline{\underline{S}}_{12}=\underline{\underline{U}}\cdot\underline{\underline{K}} \tag{10}$$

where $\underline{\underline{K}}$ is a diagonal matrix, which sets the amplitudes of the eigenvectors and is determined by inserting (10) in (7) as follows:

$$\underline{\underline{K}}=\pm\sqrt{\underline{\underline{U}}^{-1}\cdot\underline{\underline{B}}_{43}\cdot\underline{\underline{U}}^{-1^T}\cdot\left(\underline{\underline{I}}-\underline{\underline{e}}^{2\jmath\theta}\right)}. \tag{11}$$

The sign indetermination appearing in the definition of $\underline{\underline{K}}$ is due to the 180° indetermination of the scattering transmission coefficients $\underline{\underline{S}}_{12}$.

The described procedure can be carried out only if the common port supports nondegenerate modes so that all the eigenvalues λ_i are different and to each of them corresponds a one-dimensional subspace, which is spanned by the corresponding eigenvector. This constraint applies also to the procedure described in [10]. Unfortunately, the OMT common port supports two degenerate modes exhibiting the same propagation constant β so that the corresponding eigenspace is bidimensional and the eigenvectors are not uniquely defined. Therefore, the described procedure can be applied only for the evaluation of the common phase delay $\theta=\beta h$, but does not provide the $\underline{\underline{S}}_{12}$ block. For this purpose, a novel algorithm is reported in Section II-B.

B. Decomposition Algorithm

In order to evaluate the $\underline{\underline{S}}_{12}$ block of the OMT, the decomposition suggested by (4) is used. For sake of clarity, it is convenient to rewrite (4) in the more general form

$$\underline{\underline{S}}\cdot\underline{\underline{D}}\cdot\underline{\underline{S}}^{T}=\underline{\underline{B}} \tag{12}$$

where $\underline{\underline{S}}$ is the unknown matrix to be determined, $\underline{\underline{D}}$ is an unknown diagonal matrix, and $\underline{\underline{B}}$ is a known symmetric matrix. Application of the spectral decomposition to matrix $\underline{\underline{B}}$ yields

$$\underline{\underline{B}}=\underline{\underline{T}}\cdot\underline{\underline{\Lambda}}\cdot\underline{\underline{T}}^{-1} \tag{13}$$

with $\underline{\underline{\Lambda}}$ being the diagonal eigenvalue matrix of $\underline{\underline{B}}$ and $\underline{\underline{T}}$ being a matrix containing the corresponding eigenvectors. It has to be remembered [12] that, for a real symmetric matrix, the corresponding eigenvectors are orthogonal with respect to the real scalar product, i.e., with a particular choice of the eigenvectors $\underline{\underline{T}}^{T}\cdot\underline{\underline{T}}=\underline{\underline{I}}$ (the inverse matrix corresponds to its transposed matrix). Obviously, this property also holds for complex symmetric matrices even if the complex eigenvectors are not orthogonal with respect to the complex scalar product $\underline{\underline{T}}^{H}\cdot\underline{\underline{T}}\neq\underline{\underline{I}}$, denoting

$(\ldots)^H$ as the Hermitian operation. Hence, one can choose the complex amplitude of the eigenvectors so that

$$\underline{\underline{B}} = \underline{\underline{T}} \cdot \underline{\underline{\Lambda}} \cdot \underline{\underline{T}}^T. \tag{14}$$

In the remainder of this paper, the extension to the complex case of the property $\underline{\underline{T}}^T \cdot \underline{\underline{T}} = \underline{\underline{I}}$ is referred to as pseudoorthogonality. Unfortunately, matrices $\underline{\underline{\Lambda}}$ and $\underline{\underline{T}}$ differ, respectively, from matrices $\underline{\underline{D}}$ and $\underline{\underline{S}}$ appearing in (12). In fact, decomposition (14) is not unique since its most general form is

$$\underline{\underline{B}} = \underline{\underline{T}} \cdot \underline{\underline{P}} \cdot \left(\underline{\underline{P}}^{-1} \cdot \underline{\underline{\Lambda}} \cdot \underline{\underline{P}}^{-1^T} \right) \cdot \underline{\underline{P}}^T \cdot \underline{\underline{T}}^T \tag{15}$$

where $\underline{\underline{P}}$ is an unknown full matrix, which satisfies the following conditions:

$$\underline{\underline{D}} = \underline{\underline{P}}^{-1} \cdot \underline{\underline{\Lambda}} \cdot \underline{\underline{P}}^{T^{-1}} \tag{16}$$

$$\underline{\underline{S}} = \underline{\underline{T}} \cdot \underline{\underline{P}}. \tag{17}$$

Since (16) can be rewritten as

$$\underline{\underline{\Lambda}}^{-1/2} \cdot \underline{\underline{P}} \cdot \underline{\underline{D}} \cdot \underline{\underline{P}}^T \cdot \underline{\underline{\Lambda}}^{-1/2} = \underline{\underline{I}} \tag{18}$$

one can define the pseudoorthogonal matrix

$$\underline{\underline{Q}} = \underline{\underline{\Lambda}}^{-1/2} \cdot \underline{\underline{P}} \cdot \underline{\underline{D}}^{1/2} \tag{19}$$

so that

$$\underline{\underline{Q}} \cdot \underline{\underline{Q}}^T = \underline{\underline{I}}. \tag{20}$$

Using the matrix $\underline{\underline{Q}}$, (17) for the $\underline{\underline{S}}$ block becomes

$$\underline{\underline{S}} = \underline{\underline{T}} \cdot \underline{\underline{P}} = \underline{\underline{T}} \cdot \underline{\underline{\Lambda}}^{1/2} \cdot \underline{\underline{Q}} \cdot \underline{\underline{D}}^{-1/2} \tag{21}$$

where $\underline{\underline{T}}$ and $\underline{\underline{\Lambda}}$ are known matrices, whereas the pseudoorthogonal matrix $\underline{\underline{Q}}$ and diagonal matrix $\underline{\underline{D}}$ are yet to be determined. It has to be noted that the ordering of the eigenvalues $\underline{\underline{\Lambda}}$ is not required since it is taken into account in the evaluation of the matrix $\underline{\underline{Q}}$.

By applying (21) for the matrix $\underline{\underline{B}}_{21}$, obtained by considering in (4) the loads $\underline{\underline{\Gamma}}_{L,1}$ and $\underline{\underline{\Gamma}}_{L,2}$, which correspond to the reactive load connected directly and shifted by the h-long line, respectively,

$$\underline{\underline{B}}_{21} = \underline{\underline{S}}_{12} \cdot \left(\underline{\underline{e}}^{2j\theta} - \underline{\underline{I}} \right)^{-1} \cdot \underline{\underline{\Gamma}}_{L,1} \cdot \underline{\underline{S}}_{12}^T \tag{22}$$

one obtains the following expression for the $\underline{\underline{S}}_{12}$ block:

$$\underline{\underline{S}}_{12} = \underline{\underline{T}}_{21} \cdot \underline{\underline{\Lambda}}_{21}^{1/2} \cdot \underline{\underline{Q}} \cdot \underline{\underline{\Gamma}}_{L,1}^{-1/2} \cdot \left(\underline{\underline{e}}^{2j\theta} - \underline{\underline{I}} \right)^{1/2} \tag{23}$$

where $\underline{\underline{\Lambda}}_{21}$ and $\underline{\underline{T}}_{21}$ are the eigenvalues and pseudoorthogonal eigenvectors matrices of $\underline{\underline{B}}_{21}$, respectively. The common phase delay due to the line θ is computed by evaluating the average of the two eigenvalues of (8), which could be slightly different because of the measurement uncertainties. In order to derive the unknown matrices $\underline{\underline{Q}}$ and $\underline{\underline{\Gamma}}_{L,1}$, one has to consider the matrix $\underline{\underline{B}}_{43}$ defined in (7). Indeed, substitution of (23) in (7) yields

$$-\underline{\underline{\Lambda}}_{21}^{-1/2} \cdot \underline{\underline{T}}_{21}^T \cdot \underline{\underline{B}}_{43} \cdot \underline{\underline{T}}_{21} \cdot \underline{\underline{\Lambda}}_{21}^{-1/2} = \underline{\underline{Q}} \cdot \underline{\underline{\Gamma}}_{L,1}^{-1} \cdot \underline{\underline{Q}}^T. \tag{24}$$

It is to be noted that the left-hand side of (24) is a known matrix, which can be denoted by $\underline{\underline{C}}$, and that $\underline{\underline{Q}}$ is a pseudoorthogonal matrix, as stated by (20). Therefore, (24) is equivalent to

$$\underline{\underline{C}} = \underline{\underline{Q}} \cdot \underline{\underline{\Gamma}}_{L,1}^{-1} \cdot \underline{\underline{Q}}^{-1}. \tag{25}$$

From (25), it is evident that the unknown diagonal reflection coefficient matrix $\underline{\underline{\Gamma}}_{L,1}$ corresponds to the inverse of the eigenvalue matrix of $\underline{\underline{C}}$, and $\underline{\underline{Q}}$ is a proper choice of the corresponding eigenvectors matrix satisfying the pseudoorthogonality condition $\underline{\underline{Q}}^T \cdot \underline{\underline{Q}} = \underline{\underline{I}}$. The ordering of the eigenvalues of the matrix $\underline{\underline{C}}$ can be accomplished by using a rough estimate of the reflection coefficients of the reactive load $\underline{\underline{\Gamma}}_{L,1}$ (capacitive or inductive behavior) and by enforcing the continuity during a frequency sweep. Finally, the $\underline{\underline{S}}_{22}$ block can be derived by applying (3) for any value of the index i.

As a final comment to (23), it can be noticed that, in this expression, the $\underline{\underline{S}}_{12}$ block contains an indetermination concerning the following parameters:

- directions of the eigenvectors of $\underline{\underline{B}}_{21}$ (columns of $\underline{\underline{T}}_{21}$);
- signs of the square root of the eigenvalues $\underline{\underline{\Lambda}}_{21}$;
- directions of the eigenvectors of $\underline{\underline{C}}$ (columns of $\underline{\underline{Q}}$);
- signs of the square root of $\underline{\underline{\Gamma}}_{L,1}^{-1} \cdot \left(\underline{\underline{e}}^{2j\theta} - \underline{\underline{I}} \right)$.

It can be easily proven that all these factors result into a sign indetermination of the columns of $\underline{\underline{S}}_{12}$, which is typical of scattering coefficients of the transmission type. As a consequence, the off-diagonal elements of the $\underline{\underline{S}}_{22}$ block, via (3), exhibit the same indetermination. This uncertainty means that the sign of the vertical and horizontal polarizations at the common port can obviously not be determined.

III. Experimental Results

In order to evaluate the level of reliability of the algorithm, the procedure presented in Section II was applied to measure a Ka-band OMT with a 6 mm $\times$ 6 mm square waveguide as common port and standard WR28 rectangular waveguides as single-polarized ports. The load $\underline{\underline{\Gamma}}_{L,1}$ refers to a symmetrical step parallel to the waveguide walls, short circuited at a distance $s = 3.5$ mm and with aperture $c = 3.5$ mm. The step is placed at $L = 24$ mm from the reference plane, as sketched in Fig. 2. Its realization is obtained by cascading the 24-mm-long square waveguide, the 3.5-mm-thick iris, and the short circuit shown in Fig. 3. The matched load, consisting of a pyramidal absorber of lossy material ECCOSORBMF190 to be inserted in the 80-mm-long square waveguide, and the 3.5-mm-long line are reported in the same figure. Fig. 4(a) shows the measured and simulated reflection coefficients S_{11} and S_{22} at rectangular ports 1 and 2, which couple to the vertical (3) and horizontal (4) polarizations in the square port, respectively. Fig. 4(b) reports the reflection coefficients S_{33} and S_{44} relative to the vertical and horizontal polarization at the square port. The simulations were carried out by the method of moments applied in the spectral domain. In particular, the full-wave analysis of the OMT was obtained by cascading the generalized scattering matrix of each discontinuity [11]. The good agreement between the simulated and measured reflection coefficients at the common port

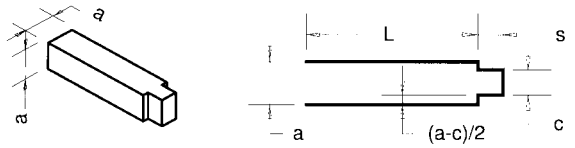

Fig. 2. Step discontinuity short circuited at a distance $s = 3.5$ mm used as reactive load $\underline{\underline{\Gamma}}_{L,1}$ in the square waveguide: $a = 6$ mm, $c = 3.5$ mm, $L = 24$ mm.

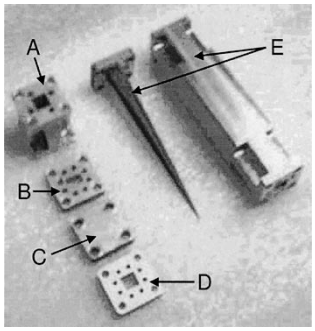

Fig. 3. Loads used in the measurements of the Ka-band OMT under test. A: 24-mm-long square waveguide. B: 3.5-mm-thick iris. C: short circuit. D: 3.5-mm-long line. E: matched load.

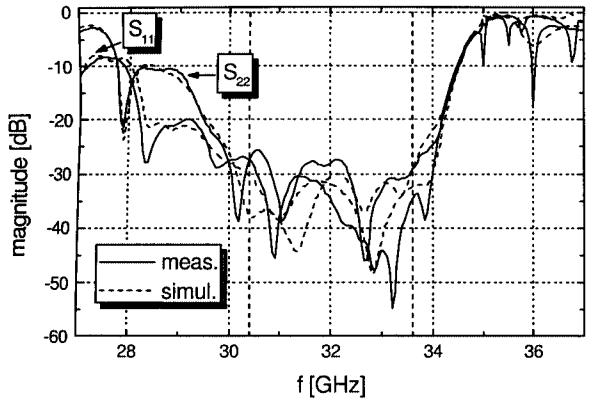

(a)

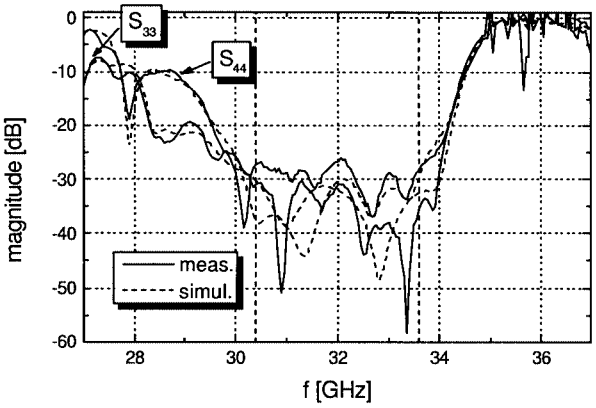

(b)

Fig. 4. Measured and simulated reflection coefficients of the Ka-band OMT under test. (a) At the two rectangular ports. (b) At the common square port (3 and 4 denote vertical and horizontal polarizations, respectively).

up to 35 GHz confirms the applicability of the presented measurement technique. It has to be noted that, for higher values of frequency, the present method starts to fail because the OMT

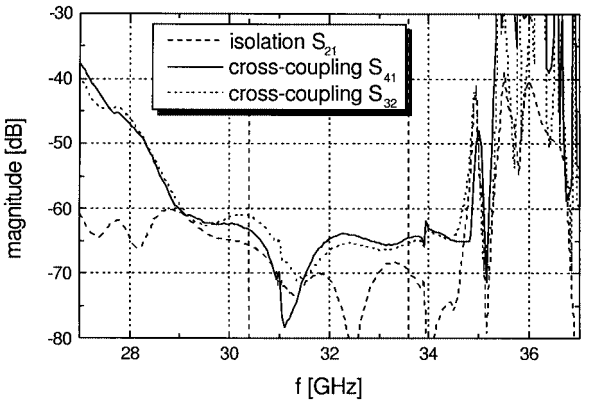

Fig. 5. Measured isolation and cross-coupling of the Ka-band OMT under test.

exhibits a high reflection coefficient at the rectangular ports for these frequencies. In this situation, the signal is mainly reflected so that the square port is almost not accessible for the electromagnetic waves excited at the rectangular ports. Hence, in this condition, it is not possible to derive accurate information about the electromagnetic behavior of the device at the common port by using only measurements performed at the rectangular ports.

Fig. 5 shows the isolation S_{21} and the cross-couplings S_{41} and S_{32} of the OMT, which are better than -60 dB in the band of interest $[30.4, 33.6]$ GHz. It has to be observed that the isolation is the off-diagonal element of the $\underline{\underline{S}}_{11}$ block, which, in this case, is directly measured by connecting the common port to a matched load. The matched load presents a residual reflection coefficient in the order of -50 dB for the diagonal elements, while its off-diagonal elements, inducing a depolarization effect, are some orders of magnitude lower. In particular, in order to measure an isolation of -70 dB, as reported in Fig. 5, the matched load must introduced a polarization coupling at the worst of the same level. This is possible by controlling the geometrical symmetry of the matched load in the square waveguide. Moreover, it was numerically verified that the diagonal/off-diagonal elements of the $\underline{\underline{S}}_{ij}$ blocks are effected by the residual values of the diagonal/off-diagonal coefficients of the matched load.

As an indicator for the measurement reliability of the presented procedure, a figure-of-merit is the agreement between the predicted and extracted reflection coefficient $\underline{\underline{\Gamma}}_{L,1}$ of the short-circuited step via the eigenvalue problem (25). As shown in Fig. 6, the simulated and measured reflection coefficients for both the vertical and horizontal polarizations are in very good agreement up to 35 GHz. In particular, in the band of interest, the maximum difference of the phase between the measurements and simulation is less than 1°. A further indicator of the quality of the procedure and standards used in the measurements is the agreement between the theoretical and measured phase delay introduced by the square waveguide. In particular, the phase delay is extracted via the eigenvalue (8). Although the two eigenvalues should be ideally identical, the measurements produce two different values of the phase delay, as shown in Fig. 7. Nevertheless, this discrepancy is less than 1° in the band of interest and the measured values agree with the theoretical one for a square

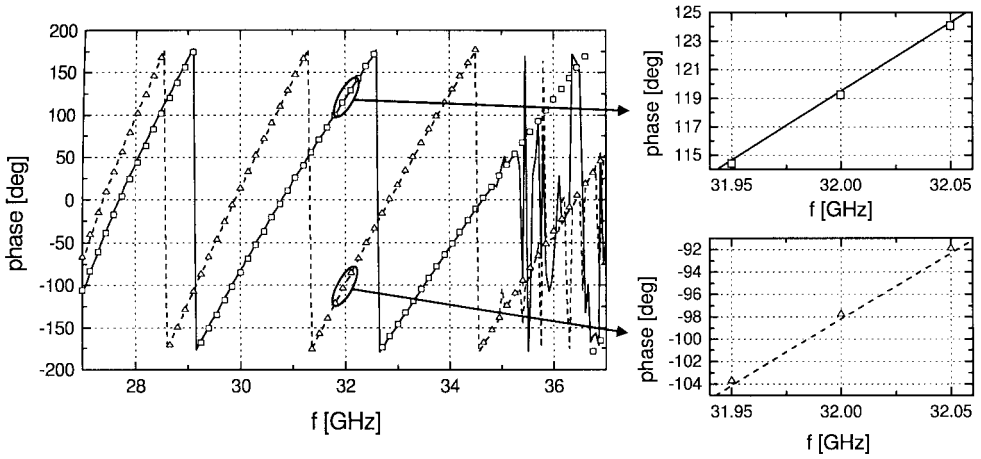

Fig. 6. Measured and simulated reflection coefficients of the short-circuited step described in the text, which was used as the load $\underline{\underline{\Gamma}}_{L,1}$ in the measurement of the Ka-band OMT under test. Dashed line: measurement—vertical polarization. Solid line: measurement—horizontal polarization. Triangles: simulation—vertical polarization. Squares: simulation—horizontal polarization.

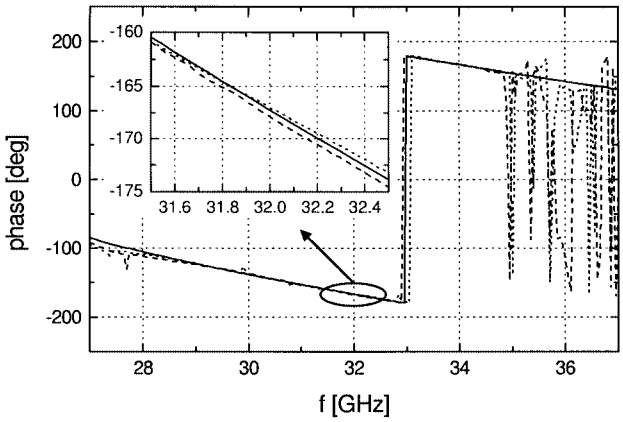

Fig. 7. Measured and simulated phase delay of the square waveguide used in the measurements of the Ka-band OMT under test. Dashed and dotted line represent the two measured values obtained as eigenvalues of (8). The solid line refers to theoretical value for a square waveguide with side $a = 5.991$ mm and length $h = 3.486$ mm (nominal values: $a = 6$ mm and $h = 3.5$ mm).

waveguide with side $a = 5.991$ mm and length $h = 3.486$ mm (nominal values: $a = 6$ mm and $h = 3.5$ mm).

IV. Conclusions

The measurement procedure that has been presented in this paper allows the full characterization of OMTs by performing a set of measurements at the single polarized ports. In this way, the network analyzer cables are maintained in the same position, avoiding a degradation of the measurement accuracy. This technique provides an accurate evaluation of the cross-coupling terms, which defines the degree of purity of the polarization at the common port, without the knowledge of multimodal standards, such as another calibrated OMT. Generally speaking, the scattering parameters involving the common port are expressed in the basis where the reflection operator of the reactive load, used as a reference, is diagonal. In particular, using the E/H-plane short-circuited steps, the scattering parameters refer to the two linear polarizations. As a further comment, we can say that an accurate characterization of OMTs, such that

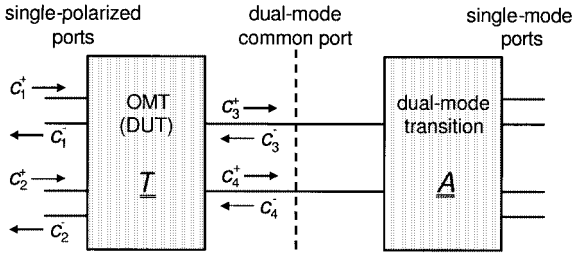

Fig. 8. Measurement setup for the evaluation of the OMT $\underline{\underline{S}}_{11}$ block.

presented in this paper, allows the realization of a multimode measurement setup useful for the experimental investigation of the cross-polarization induced by waveguide polarizers.

Appendix

As stated in Sections II and III, the $\underline{\underline{S}}_{11}$ block of the OMT can be measured by connecting a matched load to the common port. If a matched load exhibiting low values of reflection and depolarization is not available, then the $\underline{\underline{S}}_{11}$ block can be evaluated by connecting the OMT common port to an unknown dual-mode transition, as sketched in Fig. 8. This transition can be any device, which makes observable at the single-mode ports the bidimensional polarization space at the common port. Obviously, another OMT satisfies this condition. As in the TRL calibration procedure [10], two sets of measurements are performed. First, the OMT is directly connected to the transition (through) obtaining the transmission matrix

$$\underline{\underline{M}}_1 = \underline{\underline{T}} \cdot \underline{\underline{A}} \tag{26}$$

where $\underline{\underline{T}}$ and $\underline{\underline{A}}$ denote the transmission matrices of the OMT and transition, respectively. In particular, with reference to Fig. 8, the transmission matrix $\underline{\underline{T}}$ is defined as follows:

$$\begin{bmatrix} c_1^+ \\ c_2^+ \\ c_1^- \\ c_2^- \end{bmatrix} = \begin{bmatrix} \underline{\underline{T}}_{11} & \underline{\underline{T}}_{12} \\ \underline{\underline{T}}_{21} & \underline{\underline{T}}_{22} \end{bmatrix} \cdot \begin{bmatrix} c_3^+ \\ c_4^+ \\ c_3^- \\ c_4^- \end{bmatrix} \tag{27}$$

where $c_i^{\pm}$ are the amplitudes of the progressive and regressive waves at the ith port, respectively. The same definition applies also to the matrix $\underline{\underline{A}}$.

A line is then set between the two common ports and a transmission matrix $\underline{\underline{M}}_2$ is obtained such that

$$\underline{\underline{M}}_2 = \underline{\underline{T}} \cdot \underline{\underline{D}} \cdot \underline{\underline{A}} \tag{28}$$

with being D the diagonal transmission matrix of the line

$$\underline{\underline{D}} = \begin{bmatrix} \underline{\underline{e}}^{2j\theta} & \underline{\underline{0}} \\ \underline{\underline{0}} & \underline{\underline{e}}^{-2j\theta} \end{bmatrix}. \tag{29}$$

By defining the matrix

$$\underline{\underline{M}} = \underline{\underline{M}}_2 \cdot \underline{\underline{M}}_1^{-1} = \underline{\underline{T}} \cdot \underline{\underline{D}} \cdot \underline{\underline{T}}^{-1} \tag{30}$$

the transmission matrix of the OMT coincides with the eigenvectors matrix of $\underline{\underline{M}}$

$$\underline{\underline{V}} = \begin{bmatrix} \underline{\underline{V}}_{11} & \underline{\underline{V}}_{12} \\ \underline{\underline{V}}_{21} & \underline{\underline{V}}_{22} \end{bmatrix}. \tag{31}$$

As it is well known, the $\underline{\underline{S}}_{11}$ block can be written in terms of the $\underline{\underline{T}}_{11}$ and $\underline{\underline{T}}_{21}$ blocks of the transmission matrix as

$$\underline{\underline{S}}_{11} = \underline{\underline{T}}_{21} \cdot \underline{\underline{T}}_{11}^{-1} \tag{32}$$

which requires the columns of the eigenvectors matrix $\underline{\underline{V}}$ to be ordered according to (27). Although the discrimination between progressive and regressive modes is trivial, an ordering between the two degenerate progressive modes cannot be carried out and the eigenvectors are not uniquely defined. Nevertheless, a generic linear combination of the two progressive eigenvectors $\underline{\tilde{V}}_1^+$ and $\underline{\tilde{V}}_2^+$ can be expressed as

$$[\,\underline{\tilde{V}}_1^+ \quad \underline{\tilde{V}}_2^+\,] = [\,\underline{V}_1^+ \quad \underline{V}_2^+\,] \cdot \underline{\underline{L}} \tag{33}$$

where $\underline{\underline{L}}$ is any full unknown 2×2 matrix. According to (33), the $\underline{\underline{T}}_{11}$ and $\underline{\underline{T}}_{21}$ blocks can be evaluated as

$$\underline{\underline{T}}_{11} = \underline{\underline{V}}_{11} \cdot \underline{\underline{L}}, \quad \underline{\underline{T}}_{21} = \underline{\underline{V}}_{21} \cdot \underline{\underline{L}}. \tag{34}$$

Substitution of (34) in (32) leads to

$$\underline{\underline{S}}_{11} = \underline{\underline{T}}_{21} \cdot \underline{\underline{T}}_{11}^{-1} = \underline{\underline{V}}_{21} \cdot \underline{\underline{V}}_{11}^{-1} \tag{35}$$

which holds without any assumption about the matrix $\underline{\underline{L}}$. This means that the evaluation of $\underline{\underline{S}}_{11}$ does not depend on the basis used to describe the propagation in the common waveguide.

ACKNOWLEDGMENT

The authors would like to thank M. Franciotti, CMSP srl, Frossasco (Turin), Italy, for the OMT prototype manufacturing.

REFERENCES

[1] M. Ludovico, B. Piovano, G. Bertin, G. Zarba, L. Accatino, and M. Mongiardo, "CAD and optimization of compact ortho-mode transducers," *IEEE Trans. Microwave Theory Tech.*, vol. 47, pp. 2479–2486, Dec. 1999.

[2] S. J. Skinner and G. L. James, "Wide-band orthomode transducers," *IEEE Trans. Microwave Theory Tech.*, vol. 39, pp. 294–300, Feb. 1991.

[3] E. Carretti, R. Tascone, S. Cortiglioni, J. Monari, and M. Orsini, *Limits Due to Instrumental Polarization in CMB Experiments at Microwave Wavelength*, ser. New Astronomy, Elsevier Science B.V. Amsterdam, The Netherlands: Elsevier, 2001, vol. 6/3, pp. 173–188.

[4] S. Cortiglioni *et al.*, "SPOrt: A project for radio polarimetry from the international space station," presented at the STAIF 2000, Albuquerque, New Mexico, Jan. 2000.

[5] G. Chattopadhyay, B. Philhour, J. E. Carlstrom, S. Church, A. Lange, and J. Zmuidzinas, "A 96-GHz ortho-mode transducer for the Polatron," *IEEE Microwave Guided Wave Lett.*, vol. 8, pp. 421–423, Dec 1998.

[6] N. Yoneda, M. Miyazaki, and T. Noguchi, "A 90 GHz band monoblock type waveguide orthomode transducer," in *Proc. IEEE MTT-S Int. Microwave Symp. Dig.*, vol. 4, June 1999, pp. 1781–1784.

[7] G. Chattopadhyay and J. E. Carlstrom, "Finline ortho-mode transducer for millimeter waves," *IEEE Microwave Guided Wave Lett.*, vol. 9, pp. 339–341, Sept. 1999.

[8] H. J. Eul and B. Schiek, "A generalized theory and new calibration procedures for network analyzer self-calibration," *IEEE Trans. Microwave Theory Tech.*, vol. 39, pp. 724–731, Apr. 1991.

[9] R. B. Marks, "A multiline method of network analyzer calibration," *IEEE Trans. Microwave Theory Tech.*, vol. 39, pp. 1205–1215, July 1991.

[10] C. Seguinot, P. Kennis, J. F. Legier, F. Huret, E. Paleczny, and L. Hayden, "Multimode TRL—A new concept in microwave measurements: Theory and experimental verification," *IEEE Trans. Microwave Theory Tech.*, vol. 46, pp. 536–542, May 1998.

[11] T. Itoh, *Numerical Techniques for Microwave and Millimeter-Wave Passive Structures*. New York: Wiley, 1989, ch. 10.

[12] A. S. Deif, *Advanced Matrix Theory for Scientists and Engineers*. Tunbridge Wells, Kent, U.K.: Abacus Press, 1982, ch. 4.

Oscar Antonio Peverini was born in Lisbon, Portugal, in 1972. He received the Laurea degree (*summa cum laude*) in telecommunications engineering and Ph.D. degree in electronics engineering from the Politecnico di Torino, Turin, Italy, in 1997 and 2001, respectively.

From August 1999 to March 2000, he was a Visiting Member with the Applied Pysics/Integrated Optics Department, University of Paderborn, Paderborn, Germany. In February 2001, he joined the Istituto di Ricerca sull'Ingegneria delle Telecomunicazioni e dell'Informazione (IRITI), a newly established institute of the Italian National Council (CNR), Politecnico di Torino. Since December 2001, he has been a Researcher with the IRITI. His research interests include numerical simulation and design of surface acoustic wave (SAW) waveguides and interdigital transducers (IDTs) for integrated acoustooptical devices and microwave passive components and radiometers for astrophysical observations and microwave measurements techniques.

Riccardo Tascone was born in Genoa, Italy, in 1955. He received the Laurea degree in electronics engineering from the Politecnico di Torino, Turin, Italy, in 1980.

From 1980 to 1982, he was with the Centro Studi e Laboratori Telecomunicazioni (CSELT), Turin, Italy, where he was mainly involved with frequency-selective surfaces, waveguide discontinuities, and microwave antennas. In 1982, he joined the Centro Studi Propagatione e Antenne (CESPA), Turin, Italy, a laboratory of the Italian National Research Council (CNR), where he was initially a Researcher and, since 1991, a Senior Scientist (Dirigente di Ricerca). He is currently the Head of the Applied Electromagnetics Section, Istituto di Ricerca sull'Ingeneria delle Telecomunicazioni e dell'Informazione (IRITI), Politecnico di Torino, a newly established institute of the CNR. He has held various teaching positions in the area of electromagnetics with the Politecnico di Torino. His current research activities concern the areas of microwave antennas, dielectric radomes, frequency-selective surfaces, radar cross section, waveguide discontinuities, microwave filters, multiplexers, optical passive devices, and radiometers for astrophysical observations.

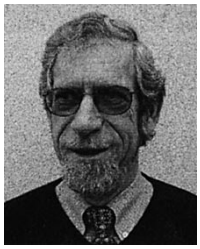

Augusto Olivieri was born in Courmayeur (AO), Italy, in 1942. He received the Diploma degree in telecommunication from the Istituto A. Avogadro di Torino, Turin, Italy, in 1963.

From 1964 to 1967, he was with Poste Telecomunicazioni e Telegrafi (PTT). From 1964 to 1971, he was a Laboratory Technician with the Department of Electronics, Politecnico di Torino. In 1971, he joined the Centro Studi Propagatione e Antenne, Turin (CESPA), Italian National Research Council (CNR). He is currently with the Istituto di Elettronica e di Ingegneria dell'Informazione e delle Telecomunicazioni (IEIIT), Turin, Italy. His primary interests cover a range of areas of telecommunication, radio propagation, antennas, measurement of microwave components, and instrumentation for advanced astrophysical observations.

Massimo Baralis was born in Turin, Italy, in 1970. He received the Laurea degree in electronics engineering from the Politecnico di Torino, Turin, Italy, in 2001.

Since May 2001, he has been with the Electromagnetics Group, Istituto di Ricerca sull'Ingegneria delle Telecomunicazioni e dell'Informazione (IRITI), Italian National Research Council (CNR), Turin, Italy. His research is focused on the application of numerical methods and measurements techniques and concerns the analysis and design of microwave and millimeter-wave passive components, feed systems, and antennas.

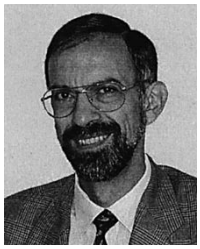

Renato Orta (M'92–SM'99) received the Laurea degree in electronics engineering from the Politecnico di Torino, Turin, Italy, in 1974.

Since 1974, he has been a member of the Department of Electronics, Politecnico di Torino, initially as an Assistant Professor, then as an Associate Professor and, since 1999, as a Full Professor. In 1985, he was a Research Fellow with the European Space Research and Technology Center (ESTEC–ESA), Noordwijk, The Netherlands. In 1998, he was a Visiting Professor (CLUSTER Chair) with the Technical University of Eindhoven, Eindhoven, The Netherlands. He currently teaches courses on EM field theory and optical components. His research interests include the areas of microwave and optical components, radiation and scattering of EM and elastic waves, and numerical techniques.

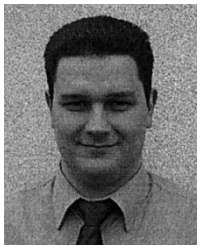

Giuseppe Virone was born in Turin, Italy, in 1977. He received the Electronic Engineering degree (*summa cum laude*) from the Politecnico di Torino, Turin, Italy, in 2001.

Since February 2002, he has been with the Applied Electromagnetics Section, Istituto di Elettronica e di Ingegneria Informatica e delle Telecomunicazioni (IEIIT), Italian National Research Council (CNR), Politecnico di Torino. His research interests are in the area of the analysis and design of microwave and millimeter-wave passive components, feed systems and antennas, waveguide discontinuities and transitions, numerical methods, and measurement techniques.